

Quantum Transparency of Anderson Insulator Junctions: Statistics of Transmission Eigenvalues, Shot Noise, and Proximity Conductance

Branislav K. Nikolić and Ralitsa L. Dragomirova

Department of Physics and Astronomy, University of Delaware, Newark, DE 19716-2570

We investigate quantum transport through strongly disordered barriers, made of materials with exceptionally high bulk resistivity that behave as an Anderson insulator or a “bad metal”, by analyzing the distribution of Landauer transmission eigenvalues for a junction where barrier is attached to two metallic leads. We find that the scaling of the transmission eigenvalue distribution with the junction thickness (starting from the single interface limit) always predicts a non-zero probability to find high transmission channels. Using this distribution, we compute the zero frequency shot noise power and demonstrate how it provides a single number characterization of non-trivial transmission properties of different types of disordered barriers. The existence of open conducting channels and corresponding violent mesoscopic fluctuations of transport quantities allows us to explain peculiar zero-bias anomalies in the Anderson-insulator/superconductor junctions observed in experiments [Phys. Rev. B **55**, 9047 (1997)]. Our findings are also relevant for the understanding of the role of extended and localized states induced by the defects that can undermine quality of thin tunnel barriers made of conventional band-insulators.

PACS numbers: 73.23.-b, 72.70.+m, 73.40.Rw

I. INTRODUCTION

The advent of mesoscopic quantum physics^{1,2} in the early 1980s has profoundly influenced our understanding of transport in solids. Advances in micro- and nano-fabrication technology have brought about small enough structures ($\lesssim 1\mu\text{m}$) in which, at low enough temperatures ($T \ll 1\text{K}$), propagation of an electron is described by a single wave function since dephasing processes can be suppressed in such systems. Thus, their transport properties have to be analyzed in terms of quantities that take into account sample-size, boundaries, and measurement set-up of macroscopic external circuit attached to the sample, rather than using traditional conductivity of bulk materials. Particularly influential ideas have emanated from the Landauer-Büttiker approach^{2,3} to quantum transport which treats conduction within the phase-coherent sample as a complicated (multichannel) quantum-mechanical scattering problem. This viewpoint introduces a set of transmission coefficients as the fundamental property of a mesoscopic conductor. The transmission coefficients T_n are formally defined as the eigenvalues of $\mathbf{t}\mathbf{t}^\dagger$, which is the product of transmission matrix \mathbf{t} and its Hermitian conjugate \mathbf{t}^\dagger . In the two-probe geometry, where mesoscopic sample is attached to two semi-infinite ideal metallic leads, the \mathbf{t} matrix connects the transmission amplitudes of the flux-normalized states in the left lead to the outgoing states in the right lead. Thus, the basis of eigenchannels, which diagonalizes the matrix $\mathbf{t}\mathbf{t}^\dagger$, offers a simple intuitive picture where conductor can be viewed as a parallel circuit of independent transmission channels characterized by channel-dependent transmission probability T_n . Within this framework, pure tunneling appears as a rather simple limit when all transmission eigenvalues become much smaller than one $T_n \ll 1$.

Since many electronic devices employ quantum-

mechanical tunneling through an insulating barrier, their design and optimization requires to understand if transport occurs via pure tunneling or if it also includes defects in the barrier. In particular, high-critical current density for Josephson tunnel junctions⁴ or impedance level for magnetic tunnel junctions⁵ require ultrathin and highly transparent barriers⁶ that can easily be pushed out of the genuine tunneling regime. The diagnostics of non-trivial barrier properties requires to investigate quantities beyond just the conductance since its exponential decrease with the barrier thickness, as a naive criterion of pure tunneling, can be generated by widely different underlying microscopic mechanisms. For example, recent experiments^{6,7} have pointed out how standard aluminum oxide barriers can accommodate high transmission channels $T_n \simeq 1$ (which are detrimental for various devices⁸), due to extended states induced by disorder rather than pinholes with more than unit-cell dimension.

When static disorder is strong enough, solids undergo localization-delocalization (LD) transition leading to an Anderson insulator.⁹ Such phase is substantially different from the conventional Bloch-Wilson band insulator since density of states at the Fermi energy remains finite in Anderson insulators. On the other hand, the wave function associated with the localized states is confined within the region of a characteristic size specified by the localization length ξ .

Here we explore quantum transport through a highly disordered barrier, separating two clean metallic electrodes, by computing statistical properties of the transmission eigenvalues for an ensemble of three-dimensional (3D) samples with different impurity configuration. We focus on the appearance of completely open transmission channels^{10,12} $T_n \simeq 1$, as the barrier thickness increases from the single interface limit to the junction thickness where tunneling through the Anderson insulator takes place, and their effect on experimentally accessible trans-

port properties. That is, the full statistics of T_n allows us to obtain frequently measured quantities that contain the signatures of such non-trivial transparency properties: (a) the zero-frequency power spectrum of the shot noise; and (b) the conductance³ G_{NS} of a hybrid junction composed of a thin Anderson insulator attached to a superconductor, whose unusual properties have been unearthed in recent mesoscopic transport experiments.¹⁰ The results on quantum transmissivity of single interface and thin barriers of a highly disordered materials are relevant also for the analogous classical scattering problems, such as the light propagation through thin, but strongly diffusive, medium.¹³

The paper is organized as follows. In Sec. II we introduce the Hamiltonian model of the disordered barrier and corresponding real-space Green function technique that allows us to obtain an exact transmission matrix of a specific sample. In Sec. III we study the scaling of the distribution of T_n as a function of the barrier thickness, where disorder strength as a parameter is set to involve both the Anderson insulator and the “bad metal” phase around the LD transition. Measurable transport quantities—shot noise and proximity conductance G_{NS} —determined by these distributions are discussed in Sec. IV. In particular, we find the shot noise to be a sensitive single parameter characterization of the transparency of multi-channel barriers, as well as of different types of diffusive transport in thick barriers. We conclude in Sec. V.

II. TRANSMISSION PROPERTIES OF THE ANDERSON MODEL FOR DISORDERED BARRIER

We model non-interacting electrons in the disordered barrier by a standard Anderson model,⁹

$$\hat{H} = \sum_{\mathbf{m}} \varepsilon_{\mathbf{m}} |\mathbf{m}\rangle \langle \mathbf{m}| + t \sum_{\langle \mathbf{m}, \mathbf{n} \rangle} |\mathbf{m}\rangle \langle \mathbf{n}|, \quad (1)$$

which is a tight-binding Hamiltonian (TBH) defined on a simple cubic lattice $L \times L_y \times L_z$. The nearest neighbor hopping matrix element, between s -orbitals $\langle \mathbf{r} | \mathbf{m} \rangle = \psi(\mathbf{r} - \mathbf{m})$ on adjacent atoms located at sites \mathbf{m} of the lattice, is denoted by t and sets the unit of energy. Here L is the thickness of the junction in the units of the lattice spacing a , i.e., the number of disordered interfaces of the cross section $L_y \times L_z$, which are stacked along the x -axis chosen as the direction of transport and coupled via hopping t to form the barrier. We set $L_y = L_z = 20$, which yields the quantum point contact conductance of the corresponding clean system attached to two leads of the same cross section as $G_{QPC}(E_F = 0) = 259G_Q$ (i.e., at half-filling there are at most 259 open conducting channels $T_n = 1$ out of 400). The disorder is introduced by setting a random on-site potential such that $\varepsilon_{\mathbf{m}}$ is uniformly distributed in the interval $[-W/2, W/2]$. The whole band of the Anderson model becomes localized (i.e., the LD transition takes place at the Fermi energy

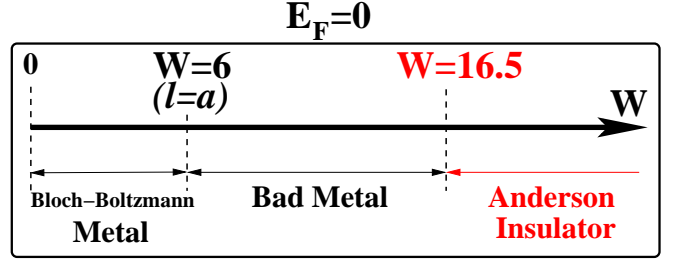


FIG. 1: The boundaries of different transport regimes, determined by the strength of the disorder W , in a bulk 3D conductor described by the half-filled ($E_F = 0$) Anderson model. At $W \approx 6$, Boltzmann theory breaks down (putative semiclassical mean free path becomes smaller than the lattice spacing $\ell \leq a$), while at $W \approx 16.5$ wave functions become localized (to observe localization effects generated by such functions, conductor has to be larger than the localization length ξ). Within the intermediate bad metal regime, particle motion is “intrinsic” diffusion that requires non-perturbative quantum description.¹⁴

$E_F = 0$ of the half-filled band) at the critical disorder strength $W_c \approx 16.5$.

It is important for subsequent discussion to recall that there are three fundamentally different transport regimes in bulk 3D disordered conductors¹⁴ (i.e., in the cubes $L \times L \times L$ with a given concentration of impurities): (a) the semiclassical regime, where Bloch-Boltzmann theory and perturbative quantum corrections (obtained from the Kubo formula) describe resistivity of diffusive systems $\ell \ll L$; (b) the “bad metal” regime characterized by exceptionally huge resistivities and lack of semiclassical mean free path ℓ (i.e., putative mean free path would be smaller than the lattice spacing $\ell < a$; nevertheless such “intrinsic” quantum diffusion can still be described by a diffusion constant extracted from the Kubo formula¹⁴)—in this regime semiclassical description and perturbative methods, based on expansion in the small parameter $1/k_F \ell$, break down; and (c) Anderson localized regime when disorder becomes strong enough that conductance of a disordered sample is smaller than³ $2e^2/h$. Figure 1 delineates the boundaries of these regimes for a system described by a half-filled Anderson model in Eq. (1).

The transmission matrix \mathbf{t}

$$\mathbf{t} = 2\sqrt{-\text{Im} \hat{\Sigma}_L} \hat{G}_{1N}^r \sqrt{-\text{Im} \hat{\Sigma}_R}, \quad (2)$$

is obtained from the real-space Green function $\hat{G}^{r,a}$

$$\hat{G}^{r,a} = \frac{1}{E - \hat{H} - \hat{\Sigma}^{r,a}}, \quad (3)$$

where \hat{G}_{1N}^r , \hat{G}_{N1}^a are submatrices of $\hat{G}^{r,a}$ ($\hat{G}^a = [\hat{G}^r]^\dagger$) that connect the layer $L = 1$ and $L = N$ of the sample along the x -axis. Here $\text{Im} \hat{\Sigma}_{L,R} = (\hat{\Sigma}_{L,R}^r - \hat{\Sigma}_{L,R}^a)/2i$ are self-energy matrices (r -retarded, a -advanced) which describe the coupling of the sample to the leads,² with

$\hat{\Sigma}^r = \hat{\Sigma}_L^r + \hat{\Sigma}_R^r$ ($\hat{\Sigma}^a = [\hat{\Sigma}^r]^\dagger$). This particular computationally efficient implementation of the Landauer-Büttker formalism, which takes microscopic Hamiltonian as an input, has its origins in the treatment of tunneling current in metal/insulator/metal (MIM) junctions that was developed in order to evade pathological properties of a tunneling Hamiltonian when attempting to take into account higher order processes.¹⁵

All of the results shown in Sec. III and Sec. IV are obtained by evaluating exactly the Landauer transmission matrix for zero-temperature quantum transport in the half-filled ($E_F = 0$) Anderson Hamiltonian Eq. (1) for a finite-size barrier. The disorder averaging is performed over an ensemble containing 1000 different samples for metallic disorder strengths $W < 16.5$ and, due to the need to search for rare events $T_n \simeq 1$ in special configurations of disorder, for 10000 samples on the insulating side $W \gtrsim 16.5$.

III. TRANSMISSION THROUGH DISORDERED INTERFACES AND THIN BARRIERS

The distribution function of the eigenvalues T_n is formally defined as

$$P(T) = \left\langle \sum_n \delta(T - T_n) \right\rangle, \quad (4)$$

where $\langle \dots \rangle$ stands for averaging over all possible realizations of impurity configurations for a given disorder strength. Most of early mesoscopic studies of phase-coherent disordered conductors has been focused on bulk systems in the weak scattering regime, where one finds celebrated perturbative quantum interference effects (such as weak localization and conductance fluctuations) within diffusive transport regime.¹ For such systems, an analytical expression for $P(T)$ has been obtained by Dorokhov¹⁶

$$P_D(T) = \frac{\langle G \rangle}{G_Q} \frac{1}{T\sqrt{1-T}}, \quad (5)$$

and rederived later on within different frameworks.^{3,17} Here $\langle G \rangle$ is the disorder-averaged conductance and $G_Q = 2e^2/h$ is the conductance quantum. The distribution $P_D(T)$ is universal in the sense that it does not depend on sample-specific properties (such as dimension, geometry, and carrier-density). Although strictly derived for a quasi-one-dimensional wire (i.e., wire whose length is much bigger than its width), the scaling of transmissions implied by $P_D(T)$ seems to have much wider validity, as long as the conductor is in (Bloch-Boltzmann) metallic regime.³

The importance of interface scattering in giant magnetoresistance phenomena has led to a reexamination of transport through disordered interfaces. For the transparency of dirty interface, whose disorder-averaged two-probe conductance is much smaller than the conductance

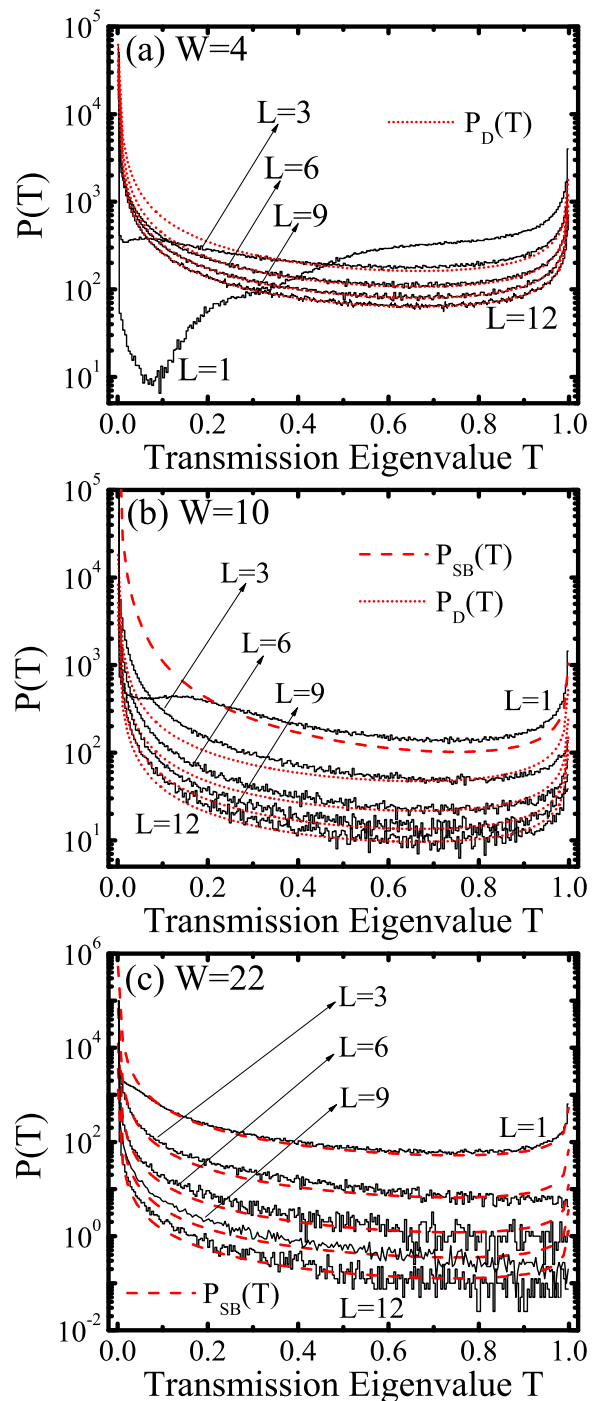


FIG. 2: The distribution of transmission eigenvalues $P(T)$ obtained in an ensemble of 1000 disordered barriers, at each junction thicknesses L . The chosen disorder strengths W of the random potential in the Anderson Hamiltonian generate the following systems in thick enough barriers (Fig. 1): (a) for $W = 4$, diffusive semiclassical metal (b) for $W = 10$, bad metal (c) for $W = 22$, Anderson insulator (here we use an ensemble of 10000 barriers). The dashed and dotted line plot the Schep-Bauer $P_{SB}(T)$ and the Dorokhov $P_D(T)$ distributions, expected to be valid for dirty interface and diffusive semiclassical metal, respectively. Note that these are not fits, but analytical expressions [see Eq. (5) and Eq. (6)] that depend on the disorder-average barrier conductance as a single parameter.

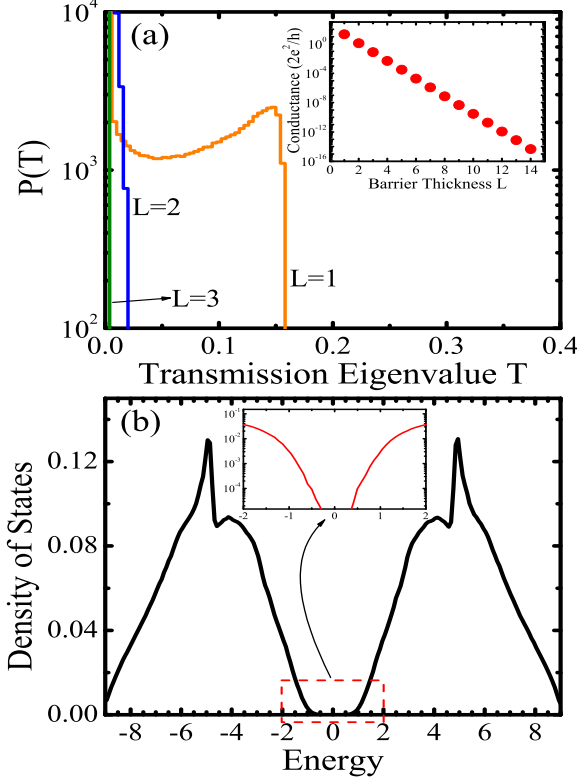


FIG. 3: The distribution of transmission eigenvalues $P(T)$ and the conductance (at $E_F = 0$) of tunnel barriers of different thickness that are made of disordered binary alloy $A_{0.5}B_{0.5}$ [panel (a)]. The binary alloy is modeled by the Anderson Hamiltonian Eq. (1) with $\varepsilon_A = -\varepsilon_B = 4.6$ being randomly distributed on its diagonal. This random potential energy induces a hard gap in the eigenspectrum around $E_F = 0$, as shown in the panel (b). Such gap is phenomenologically similar to the gap in the density of states of band or Mott insulators.

of corresponding point contact $\langle G \rangle < G_{QPC}$, a Schep-Bauer distribution¹⁹ has been found to be applicable

$$P_{SB}(T) = \frac{\langle G \rangle}{\pi G_Q} \frac{1}{T^{3/2} \sqrt{1-T}}. \quad (6)$$

While $P_{SB}(T)$ has been derived in the limit where barrier thickness is much smaller than the Fermi wavelength λ_F , recent experiments⁷ have suggested that it might be valid even for thicker strongly disordered barrier $\lambda_F \ll L < \xi$, on the proviso that its width is smaller than the localization length ξ .

Besides diffusive wires and dirty interfaces, analytical expression for $P(T)$ has been derived for chaotic cavities and double barrier junctions, as well as for combinations of these four generic cases.³ Despite important insights obtained from different approaches^{3,16,17,19} that yield $P_D(T)$ and $P_{SB}(T)$, no theory exist that would makes it possible to obtain analytical expression for $P(T)$ of a 3D mesoscopic disordered conductor that is in the non-semiclassical diffusive regime (i.e., the bad metal in

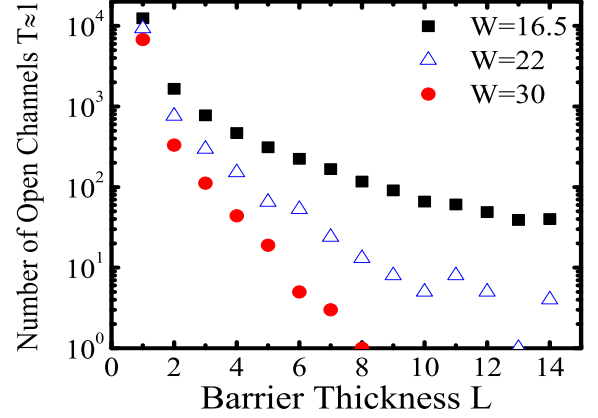


FIG. 4: The number of open channels $T_n \in [0.95, 1]$ in an ensemble of 1000 barriers for a given junction thickness. The barriers are made of highly disordered materials, characterized by the disorder strength $W = \{16.5, 22, 30\}$, which behaves as the Anderson insulator in the bulk (see related Fig. 1 and Fig. 2).

Fig. 1), and extending all the way into the localized regime.³ Therefore, we plot in Fig. 2 *numerically exact* $P(T)$ as a function of the barrier thickness, obtained by diagonalizing $\mathbf{t}\mathbf{t}^\dagger$ in Eq. (2) for each sample of an ensemble of disorder configurations. For thick enough, metallic $\ell \ll L \ll \xi$ (quasi-one-dimensional system become insulators when $L > \xi$ independently of the strength of the disorder³), barriers where semiclassical diffusive transport takes place [panel (a)], $P_D(T)$ accounts well for the transmission eigenvalue distribution. However, for barriers made of the bad metal, $P(T)$ is not equal to either $P_D(T)$ or weak-localization corrected²³ $P_D(T)$, even though it remains bimodal distribution with most of channels being either closed $T_n \simeq 0$ or open $T_n \simeq 1$ [panel (b)]. Note that no single interface in the metallic range of disorder strengths $W \lesssim 16.5$ is well described by $P_{SB}(T)$ [panels (a) and (b)].

When the disorder is strong enough to drive the LD transition in the bulk 3D samples, $P_{SB}(T)$ becomes valid in the single plane limit [panel (c)]. Moreover, it is also useful to some extent to describe $P(T)$ for barriers composed of few such planes, as suggested by experiment and semi-intuitive arguments of Ref. 7. Finally, in Sec. IV we demonstrate that the shot noise provides very sensitive tool to compare different distributions $P(T)$ encountered here, as well as to differentiate those that might appear to be similar [e.g., the distributions in panel (c)]. This is due to the fact that non-trivial features of $P(T)$, such as the appearance of open channels in disordered tunnel barrier,^{6,10} directly affect the suppression of the shot noise power below its value in the pure tunneling limit.

To contrast the transport through highly disordered barriers with tunneling through barriers made of a material with a gap in the density of states (such as the conventional band-insulators determined by single-particle

quantum mechanics,⁶ or the “esoteric” Mott insulators determined by strongly correlated physics²⁴), we introduce disordered binary alloy $A_{0.5}B_{0.5}$ between the metallic leads. This system, which is composed of an equal number of atoms A and B randomly distributed throughout the simple cubic lattice, is modeled by random potential energy $\varepsilon_A = -\varepsilon_B$ on the diagonal of TBH in Eq. (1). As shown in Fig. 3, large enough $\varepsilon_A = |\varepsilon_B|$ will open a hard gap around $E_F = 0$ in the density of states (DOS). The single interface of a solid with the gap in the bulk DOS can display distinctive transport properties,²⁴ which manifest here as a non-trivial distribution of transmission eigenvalues where not all T_n are negligible. However, already for the ultrathin barriers $L = 4$, all transmission eigenvalues drop into the interval $T_n \in [0, 0.004]$, while the conductance follows typical exponential decay as a function of L .

On the other hand, the disordered barriers always display a non-trivial distribution of transmission eigenvalues, which can accommodate open channels even at very large W and beyond the ultrathin limit. In the case of single interfaces and ultrathin barriers, the disordered region does not provide enough spatial extension in the transport direction to allow for the localization of wave functions¹⁹ (which is also leads to emergence of the low-energy extended states within disordered ultrathin aluminum oxide barriers⁶). We plot in Fig. 4 the decay of the number of open channels as the barrier thickness increases, where the disorder strengths correspond to the Anderson insulator in Fig. 1. The appearance of open channels beyond ultrathin barrier widths is a type of a rare event in the Anderson insulating phase, which is analogous to other rare events that can arise in special disorder configurations of disorder, even in the metallic phase.²⁶

When Anderson insulator samples are bigger than the inelastic scattering length L_ϕ , phonon-assisted tunneling allows charges to propagate by hopping between the localized sites, thereby generating finite conductance. However, the transport studied here takes place through phase-coherent barriers (which are smaller than L_ϕ and, therefore, effectively at zero temperature). The open channels inside the Anderson insulator junctions are due to the tunneling via rather special configurations of localized states that provide a path for resonant transmission of electrons.²⁵ One example of such rare event is a wave function, with energy close to the Fermi energy ($E_F = 0$), which is symmetric with respect to the leads. Such wave function would make possible resonant transmission $T_n \simeq 1$, so that the conductance is proportional to the probability of finding such special barrier. This can be seen by comparing Fig. 4 (which essentially gives the probability to encounter an open channel in a given ensemble of barriers) to the corresponding barrier conductances plotted in Fig. 6.

IV. LINEAR STATISTICS: SHOT NOISE AND PROXIMITY CONDUCTANCE

Over the past decade experimental and theoretical investigation of the shot noise, as a random process characterizing non-equilibrium state into which a phase-coherent conductor is driven by the applied voltage, has become an active frontier of mesoscopic physics. The power spectrum of the shot noise, at zero frequency and at zero temperature, can be expressed¹¹ in terms of the Landauer transmission eigenvalues T_n for non-interacting electrons transported through a conductor attached to two leads

$$S = 2 \int_{-\infty}^{+\infty} dt' [\overline{I(t)I(t')} - \bar{I}^2] = 2eV \frac{2e^2}{h} \sum_{n=1}^{L_y \times L_z} T_n(1-T_n). \quad (7)$$

Here \bar{I} is the time-average of the current flowing through the system under the applied voltage V . Thus, by measuring the shot noise one effectively probes second moment of $P(T)$, thereby obtaining complementary information to traditional conductance that is associated with the first moment of $P(T)$.

The suppression of the shot noise power $S = 2Fe\bar{I}$ with respect to the Poisson limit $S = 2e\bar{I}$ is quantified by the Fano factor F . In the pure tunneling regime $T_n \ll 1 \Rightarrow F = 1$ because transfer of electrons through the barrier is uncorrelated in time and, therefore, described by the Poisson statistics. On the other hand, in the diffusive metallic conductors (more precisely, in the disordered Bloch-Boltzmann conductors in Fig. 1 whose size is such that $\ell \ll L$), the shot noise power is reduced by a factor¹¹ $F = 1/3$. This is due to the correlations generated by Fermi statistics—electron injection into the conductor is less likely if another electron is already occupying one of the conducting channels. In the ballistic limit $T_n = 1$, Pauli principle correlating non-interacting fermions leads to a complete noise suppression $F = 0$. The shot noise is a genuine quantum transport phenomenon since deterministic classical transport also suppresses S to zero due to the lack of stochasticity associated with quantum mechanical propagation of electrons. The “magic” suppression factors, such as $F = 1/3$, are expected to be universally valid, i.e., independent on the details of the system such as geometric parameters of the conductor or its resistance. Since $F = 1/3$ follows from $P_D(T)$ used in Eq. (7), while $P_{SB}(T)$ gives $F = 1/2$, the Fano factors may serve as an indirect and experimentally observable confirmation of a particular distribution $P(T)$.

The knowledge of $P(T)$ makes it possible to compute the disorder-average of any quantity that can be cast into a form of the so-called linear statistics $A = \sum_n a(T_n)$

$$\langle A \rangle = \left\langle \sum_n a(T_n) \right\rangle = \int dT a(T) P(T). \quad (8)$$

The most frequently investigated examples of such quan-

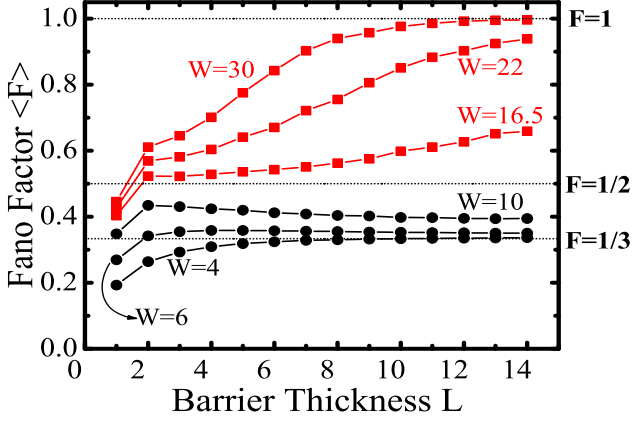


FIG. 5: The disorder-averaged Fano factor, quantifying suppression of the shot noise power $S = 2FeI$ from its Poisson value $F = 1$, as a function of the barrier thickness. Each curve is parametrized by the strength of the disorder W introduced in barrier (see Fig. 1). Note that the three horizontal lines label: (i) $F = 1/3$ shot noise suppression expected in the diffusive semiclassical conductors [i.e., Bloch-Boltzmann metal in Fig. 1 whose transparency is described by $P_D(T)$]; (ii) $F = 1/2$ for dirty interfaces described by $P_{SB}(T)$; and (iii) $F = 1$ as a signature of pure tunneling through an insulator.

ties,³ measured in the two-probe geometry and at zero-temperature, are:

(a) the Landauer conductance

$$\langle G \rangle = \frac{2e^2}{h} \left\langle \sum_n T_n \right\rangle = \frac{2e^2}{h} \int dT T P(T), \quad (9)$$

(b) the Fano factor

$$\langle F \rangle = \frac{\langle \sum_n T_n (1 - T_n) \rangle}{\langle \sum_n T_n \rangle} = \frac{\int dT T (1 - T) P(T)}{\int dT T P(T)}, \quad (10)$$

(c) the linear conductance of a normal-region/superconductor (NS) junction

$$\begin{aligned} \langle G_{NS} \rangle &= \frac{2e^2}{h} \left\langle \sum_n \frac{2T_n^2}{(2 - T_n)^2} \right\rangle \\ &= \frac{2e^2}{h} \int dT \frac{2T^2}{(2 - T)^2} P(T). \end{aligned} \quad (11)$$

The proximity effect, which modifies the conductance of the N region, is microscopically generated by Andreev reflection processes at the NS interface. The expression for $\langle G_{NS} \rangle$ is obtained by taking into account these processes within Bogoliubov-De Gennes equations framework while neglecting the self-consistency issues³ (i.e., superconducting order parameter is assumed to be a step function, which evades analyzing its depression on the S side of the junction²⁰). Also, when mesoscopic conductor is sandwiched between two superconductors, the subharmonic gap structure of the $I - V$ characteristic of

such Josephson junction is determined²¹ by $P(T)$, which has recently been utilized as an experimental probe of the transmission properties of atomic²² and mesoscopic conductors.⁷

Figure 5 demonstrates that $F = 1/3$ suppression is indeed applicable in the Bloch-Boltzmann transport regime, i.e., in the transport through thick enough barriers (but still $L < L_y, L_z$) where semiclassical diffusive ($\ell \ll L$) charge propagation takes place. Moreover, the suppression factor shows saturation behavior as a function of the barrier thickness $\langle F(L) \rangle \rightarrow F_M$ also for diffusion through the bad metal barrier. However, its asymptotic value F_M is steadily increasing $F_M > 1/3$ as a function of W when $W \gtrsim 6$. For the Anderson insulator barriers $W \gtrsim 16.5$, the Fano factor is $1/3 < \langle F(L) \rangle < 1$, as long as there is a probability to encounter open channels (Fig. 4) through the barrier. It is also monotonic function of the barrier thickness since $P(T)$ scales with L in a fashion shown in panel (c) of Fig. 2. When all channels become closed in thick Anderson insulator barriers, the Fano factor reaches its trivial asymptotic value $\langle F \rangle = 1$, thereby signaling that pure tunneling takes place through such Anderson insulator barriers. Thus, Fig. 5 suggests that the Fano factor offers a unique single scalar quantity that is able to resolve disordered thin barriers with different transmission properties, as well as to label diffusive transport regimes of Fig. 1 within thick barriers.

The possibility of fully open channels $T = 1$ to exist in the Anderson insulator barriers, which we have demonstrated in Sec. III, has been indicated previously in the measurements of zero-bias anomaly in the $I - V$ characteristic of normal-metal/Anderson-insulator/superconductor (NIS) junctions.¹⁰ Furthermore, the comparison of the conductance $\langle G_{NS} \rangle$ of NIS junction with the conductance of the barrier itself $\langle G \rangle$ (i.e., $\langle G \rangle$ is the conductance of the metal/Anderson-insulator/metal junction) allows one to test the importance of different special configurations of localized states that allow for resonant tunneling and, therefore, increase the zero-bias conductance. For example, in the case of resonant tunneling through a chain of two localized sites, $\langle G_{NS} \rangle \approx 0.27 \langle G \rangle$. The same trend was conjectured to persist in barriers where tunneling through quasi-one-dimensional chains of arbitrary number of localized states occurs.²⁷ As the thickness of the barrier increases, more complex configurations become possible. However, they have not been observed in experiments measuring the normal conductance $\langle G \rangle$. Nevertheless, experiments¹⁰ on NS junctions find $G_{NS}/G \in [1.5, 3.5]$. Moreover, purely Andreev processes at a perfectly transparent NS interface set the maximum at $G_{NS}/G = 2$ (which is the ratio of Eq. (11) and Eq. (9) for $T_n = 1$).

Figure 6 plots the conductance of the Anderson insulator junctions, as well as the corresponding ratio $\langle G_{NS} \rangle / \langle G \rangle$ when one of the normal leads of the MIM junction is turned into a superconducting one. The distributions of $P(T)$ obtained in Sec. III yields $\langle G_{NS} \rangle / \langle G \rangle \in [0.4, 0.6]$ as a function of the barrier thickness. However,

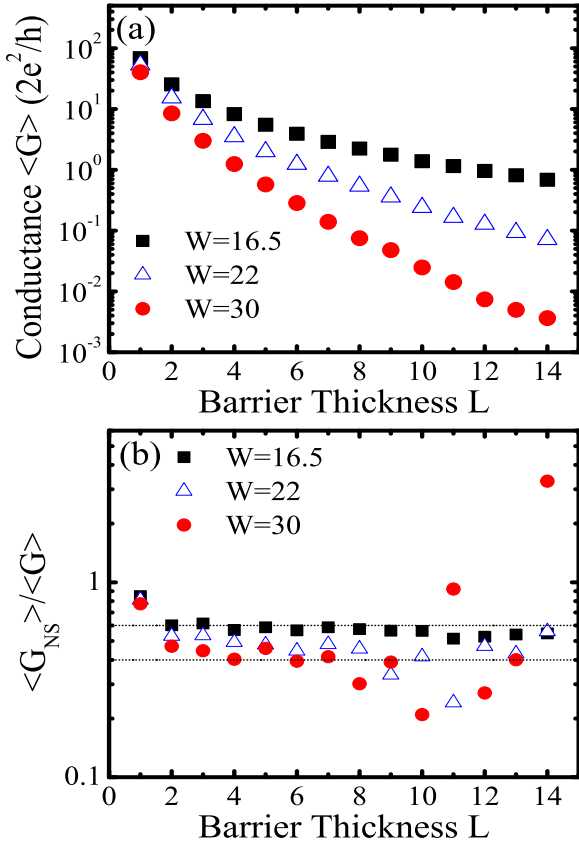


FIG. 6: The disorder-averaged conductance of the Anderson insulator junctions of different thickness, attached to two metallic leads [panel (a)]. The panel (b) plots the ratio $\langle G_{NS} \rangle / \langle G \rangle$ of the disorder-averaged linear conductance of a normal-region/superconductor junction [where normal-region is the barrier from panel (a)] and $\langle G \rangle$ from panel (a).

we recall that the study of full distribution functions of equilibrium and kinetic quantities has been one of the key concepts introduced by mesoscopic program.¹ In particular, conductance fluctuations in highly disordered phase-coherent samples can reach the same magnitude as the conductance itself.^{3,28} Therefore, we investigate G_{NS}/G for each sample within our impurity ensemble at a given barrier thickness. As shown in Fig. 7, particular phase-coherent samples can indeed exhibit $0.27 < G_{NS}/G < 2$, similarly to the ones found in experiments.¹⁰ Therefore, it seems plausible that peculiar samples with $G_{NS}/G > 2$ of Ref. 10 stem either from experimental artifacts (such as the procedure for measuring¹⁰ G) or from processes that are not captured by Eq. (11) that takes into account only Andreev reflection at the NS interface.

V. CONCLUSION

We have investigated how statistics of Landauer transmission eigenvalues $P(T)$ for 3D highly disordered bar-

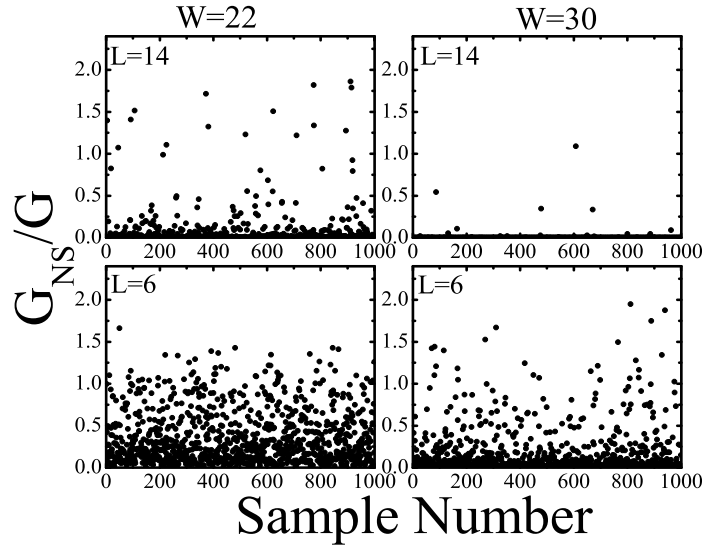


FIG. 7: Mesoscopic sample-to-sample fluctuations of G_{NS}/G (see Fig. 6) for the Anderson insulator barriers characterized by the disorder strength $W = \{22, 30\}$ and thickness $L = \{6, 14\}$

riers attached to two ideal metallic leads scales with the thickness of the barrier. When barriers are made of the bad metal (characterized by exceptionally high resistivity and lack of mean free path), $P(T)$ remains bimodal, but it does not obey scaling predicted by the standard Dorokhov distribution (whose validity is confined to the semiclassical diffusive metallic transport regime). The distributions of all metallic (semiclassical or quantum) diffusive barriers is indirectly captured by the scale independent Fano factor $F \geq 1/3$ measuring suppression of the shot noise power. In special configuration of disorder, Anderson insulator barrier allow for the existence of open channels $T_n = 1$ due to resonant trajectories through localized states, which makes it possible to encounter thin MIM junctions with $F < 1$, or normal-metal/Anderson-insulator/superconductor junctions with $0.27 < G_{NS}/G < 2$.

Acknowledgments

We thank Z. Ovadyahu and J. K. Freericks for enlightening discussions and L. P. Zârbo for help.

-
- ¹ *Mesoscopic Phenomena in Solids*, edited by B.L. Altshuler, P.A. Lee, and R.A. Webb (North-Holland, Amsterdam, 1991).
 - ² S. Datta, *Electronic transport in mesoscopic systems* (Cambridge University Press, Cambridge, 1995).
 - ³ C.W.J. Beenakker, *Rev. Mod. Phys.* **69**, 731 (1997).
 - ⁴ M. Gurvitch, M.A. Washington, and H.A. Huggins, *Appl. Phys. Lett.* **42**, 472 (1983).
 - ⁵ J.S. Modera and G. Mathon, *J. Magn. Magn. Mater.* **200**, 248 (1999).
 - ⁶ W. H. Pippard, A.C. Perella, F.J. Albert, and R.A. Buhrman, *Phys. Rev. Lett.* **88**, 046805 (2002).
 - ⁷ Y. Naveh, V. Patel, D.V. Averin, K.K. Likharev, and J.E. Lukens, *Phys. Rev. Lett.* **85**, 5404 (2000).
 - ⁸ E.P. Price, D.J. Smith, R.C. Dynes, and A.E. Berkowitz, *Appl. Phys. Lett.* **80**, 285 (2002).
 - ⁹ P.W. Anderson, *Phys. Rev. B* **109**, 1492 (1958).
 - ¹⁰ A. Frydman and Z. Ovadyahu, *Phys. Rev. B* **55**, 9047 (1997).
 - ¹¹ Ya.M. Blanter and M. Büttiker, *Phys. Rep.* **336**, 1 (2000).
 - ¹² Y. Asano, *Phys. Rev. B* **66**, 174506 (2002).
 - ¹³ M. Patra, *Phys. Rev. E* **67**, 016603 (2003).
 - ¹⁴ B. K. Nikolić and P. B. Allen, *Phys. Rev. B* **63**, R020201 (2001).
 - ¹⁵ C. Caroli, R. Combescot, P. Nozieres, and D. Saint-James, *J. Phys. C* **4**, 916 (1971).
 - ¹⁶ O. N. Dorokhov, *Pis'ma Zh. Éksp. Teor. Fiz.* **36**, 259 (1982) [*JETP Lett.* **36**, 318 (1982)].
 - ¹⁷ A.V. Tartakovski, *Phys. Rev. B* **52**, 2704 (1995).
 - ¹⁸ M.A.M. Gijs and G.E.W. Bauer, *Adv. Phys.* **46**, 113 (1997); P. Zahn, J. Binder, I. Mertig, R. Zeller, and P.H. Dederichs, *Phys. Rev. Lett.* **80**, 4309 (1998).
 - ¹⁹ K.M. Schep and G.E.W. Bauer, *Phys. Rev. Lett.* **78**, 3015 (1997).
 - ²⁰ B.K. Nikolić, J.K. Freericks, and P. Miller, *Phys. Rev. B* **64**, 212507 (2001).
 - ²¹ A. Bardas and D.V. Averin, *Phys. Rev. B* **56**, 8518 (1997).
 - ²² E. Scheer, P. Joyez, D. Esteve, C. Urbina, and M.H. Devoret, *Phys. Rev. Lett.* **78**, 3535 (1997).
 - ²³ Yu.V. Nazarov, *Phys. Rev. B* **52**, 4720 (1995).
 - ²⁴ J.K. Freericks, *Appl. Phys. Lett.* **84**, 1383 (2004).
 - ²⁵ M. Naito and M.R. Beasley, *Phys. Rev. B* **35**, 2548 (1987).
 - ²⁶ B.K. Nikolić, *Phys. Rev. B* **65**, 012201 (2002).
 - ²⁷ I.L. Aleiner, P. Clarke, and L.I. Glazman, *Phys. Rev. B* **53**, 7630 (1996).
 - ²⁸ F. P. Milliken and Z. Ovadyahu, *Phys. Rev. Lett.* **65**, 911 (1990).